

Supporting Information

Ultrapерmeable Nanofiltration Membranes with Tunable Selectivity Fabricated with Polyaniline Nanofibers

Chenhao Ji,^{a,b,c} Cheng-Wei Lin,^b Shenghao Zhang,^c Yaoli Guo,^a Zhe Yang,^{a,c} Weiping Hu,^c
Shuangmei Xue,^{a,b,c,*} Q. Jason Niu,^{a,c,*} Richard B. Kaner^{b,*}

^a College of Civil and Transportation Engineering, Shenzhen University, Shenzhen 518060, China

^b Department of Chemistry and Biochemistry and California NanoSystems Institute, University of California, Los Angeles, Los Angeles, California 90095, United States

^c Institute for Advanced Study, Shenzhen University, Shenzhen 518060, China

* To whom all correspondence should be addressed.

* E-mail: xueshuangmei999@gmail.edu (S. Xue).

* E-mail: qjasonniu@szu.edu.cn (Q. Jason Niu).

* E-mail: kaner@chem.ucla.edu (R. B. Kaner).

Table of Contents

Figure S1. Surface and cross-sectional morphology of the PES microfiltration membrane used as the support membrane.

Figure S2. The crossflow device for evaluating the nanofiltration performance.

Figure S3. The morphology of the synthesized PANI nanofiber.

Figure S4. The thickness of PANI interlayer as a function of the PANI nanofiber's loading.

Figure S5. Color change of the PANI interlayer during the interfacial polymerization process: (a, b, c) U-*i*TFC-1%, (d, e, f) U-*i*TFC-0.05%, (g, h, i) D-*i*TFC-1%, and (j, k, l) D-*i*TFC-0.05%.

Figure S6. Comparison of the systematical stability of (a) HCl molecules are dissociative, (b) HCl molecules are all bonded with PIP monomers, (c) HCl molecules are bonded both with PIP monomers and PANI and (d) HCl molecules are solely bonded with PANI.

Figure S7. Additional SEM images to **Fig. 3** showing the surface and cross-sectional morphology of D-*i*TFC-1% and D-*i*TFC-0.05%.

Figure S8. PA films supported on silicon wafers for thickness measurements.

Figure S9. Elemental mapping of the positions marked with a red dot in **Fig. 4c** and **Fig. 4d**.

Table S1. EDX elemental distribution of **Fig. S9a**.

Table S2. EDX elemental distribution of **Fig. S9b**.

Figure S10. Surface and cross-sectional morphology of the *i*TFC membrane of which the PANI interlayer is prepared with a 2 mg cm⁻² loading of PANI nanofibers.

Figure S11. C1s high resolution XPS spectra of TFC-C, U-*i*TFC-1%, D-*i*TFC-1%, U-*i*TFC-0.05%, and D-*i*TFC-0.05%.

Figure S12. Surface and cross-sectional morphology of (a, b, c) TFC-C-UF and (d, e, f) U-*i*TFC-1%-UF.

Figure S13. EDX measurement of (a) emeraldine base and (b) emeraldine salt PANI nanofibers with (c) and (d) as the elemental mapping, respectively.

Table S3. Elemental distribution of emeraldine base PANI nanofiber.

Table S4. Elemental distribution of emeraldine salt PANI nanofiber.

Figure S14. A comparison of Na₂SO₄ rejection and PWF of *i*TFC membranes with PANI interlayers in this work to *i*TFC membranes with other materials-based interlayers.

Figure S15. Long-term stability test of nanofiltration.

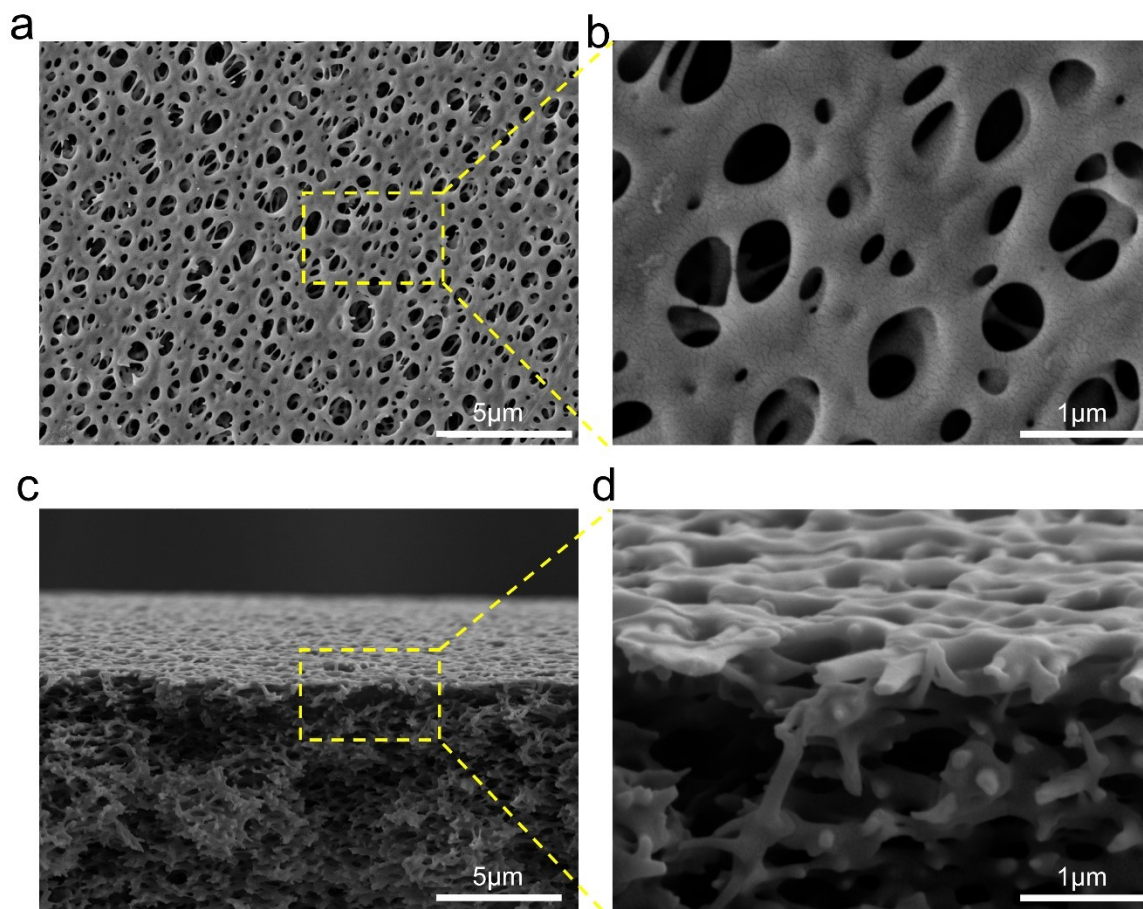


Figure S1. Surface and cross-sectional morphology of the PES microfiltration membrane used as the support membrane.

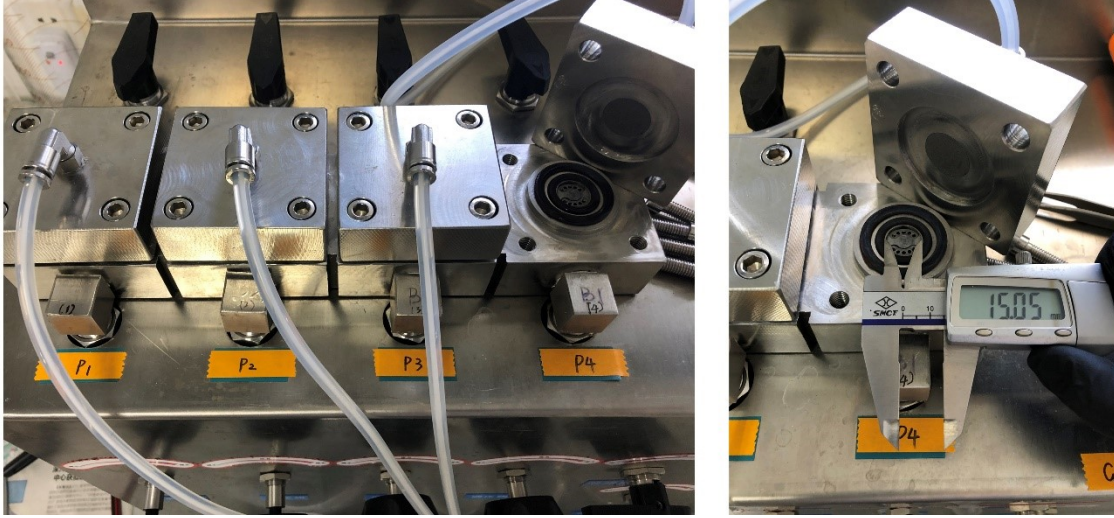


Figure S2. The crossflow device for evaluating the nanofiltration performance.

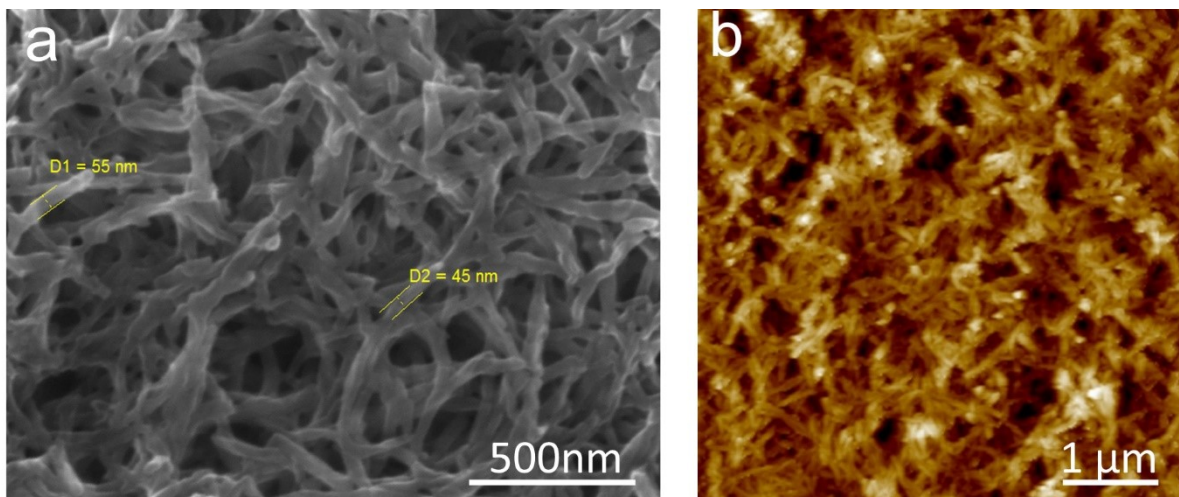


Figure S3. The morphology of the synthesized PANI nanofibers.

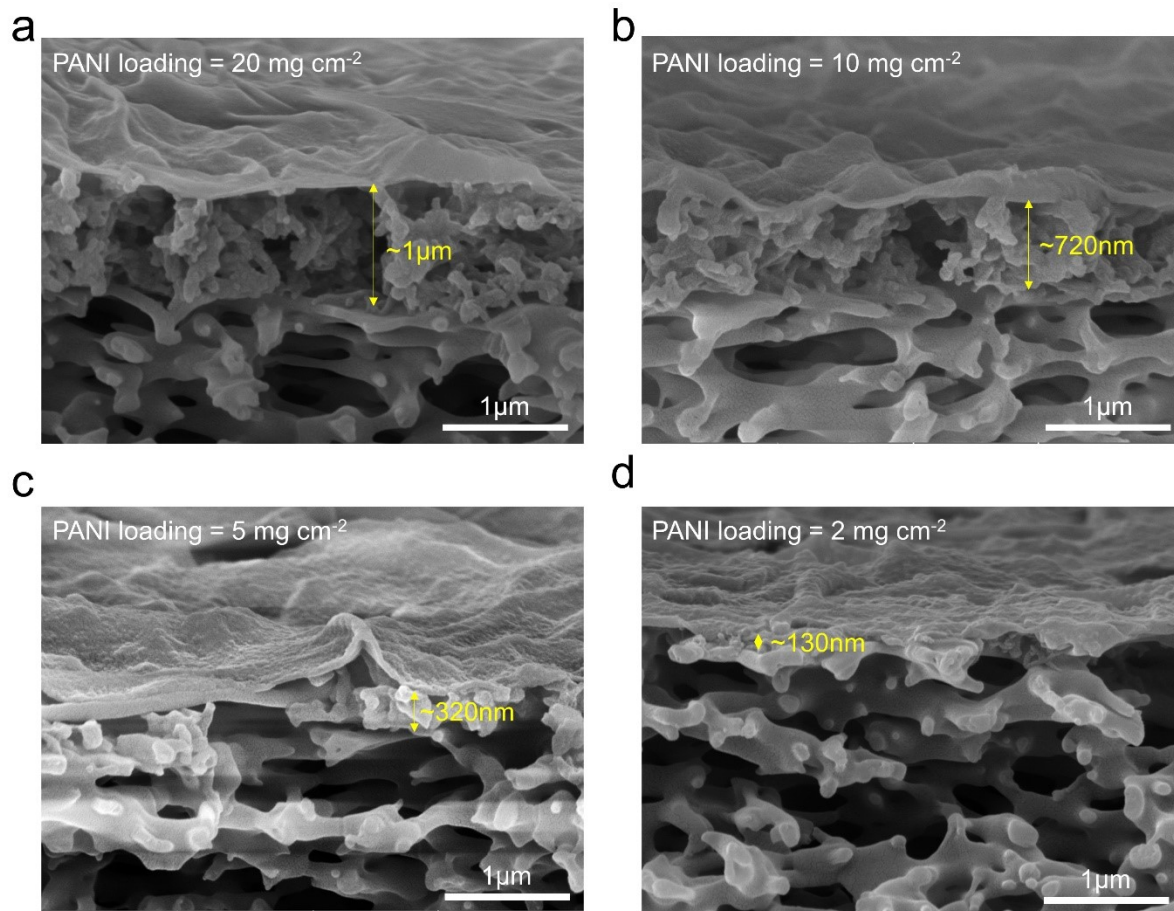


Figure S4. The thickness of PANI interlayer as a function of the PANI nanofiber loading.

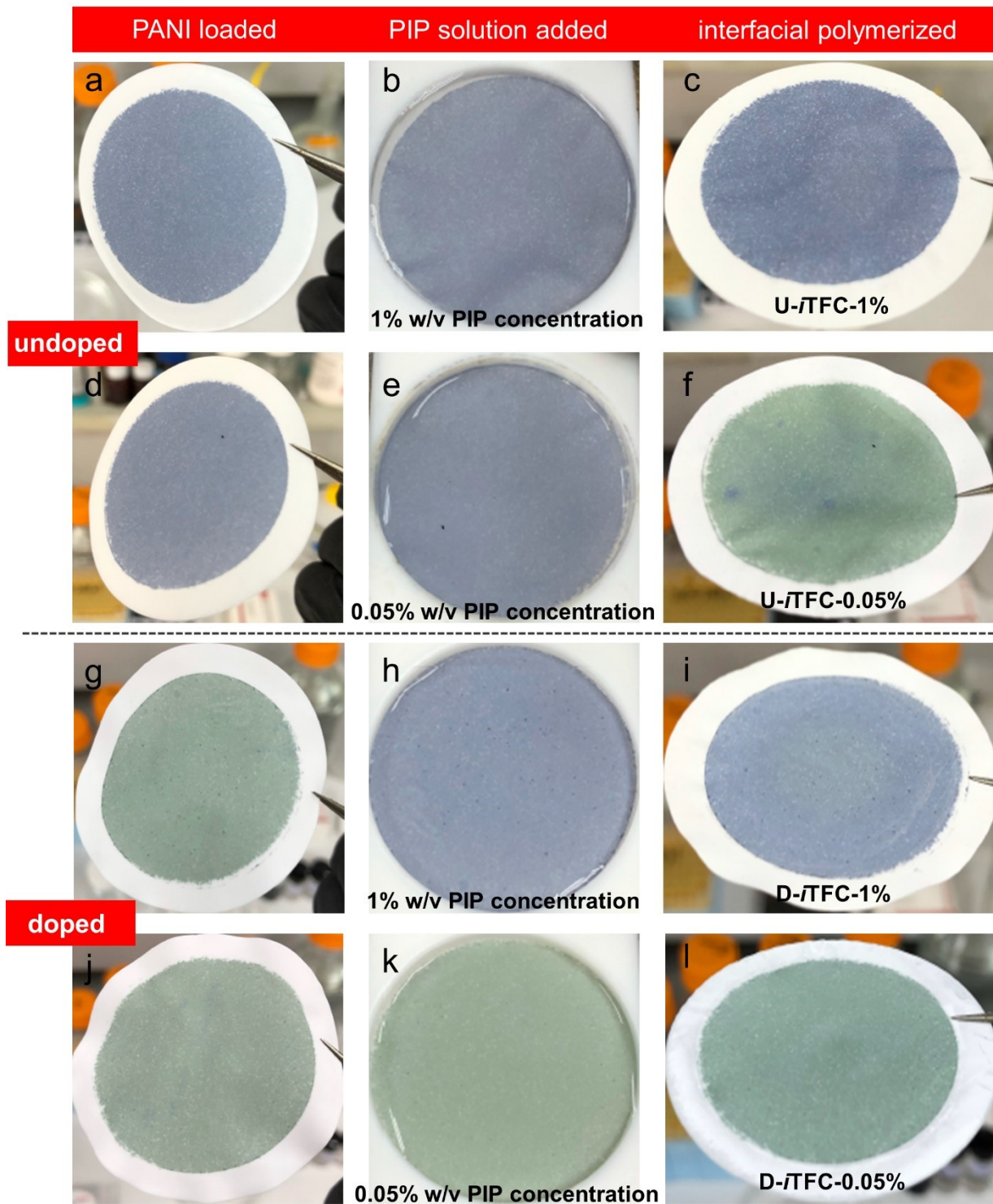


Figure S5. Color change of the PANI interlayer during the interfacial polymerization process: (a, b, c) U-*i*TFC-1%, (d, e, f) U-*i*TFC-0.05%, (g, h, i) D-*i*TFC-1%, and (j, k, l) D-*i*TFC-0.05%.

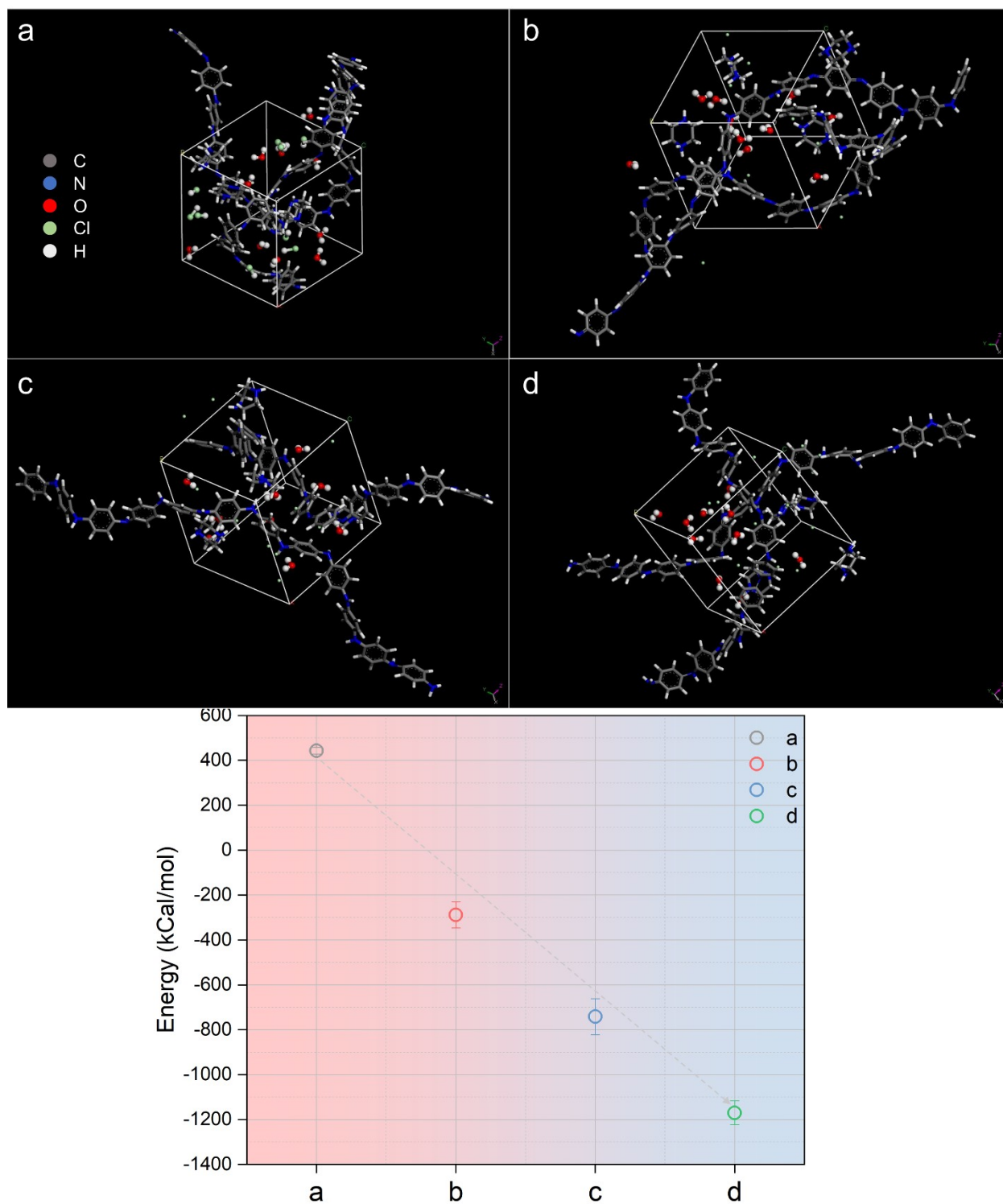


Figure S6. Comparison of the stability when (a) the HCl molecules are dissociative, (b) the HCl molecules are all bonded to the PIP monomers, (c) the HCl molecules are bonded both to the PIP monomers and to the PANI and (d) HCl molecules are solely bonded to the PANI.

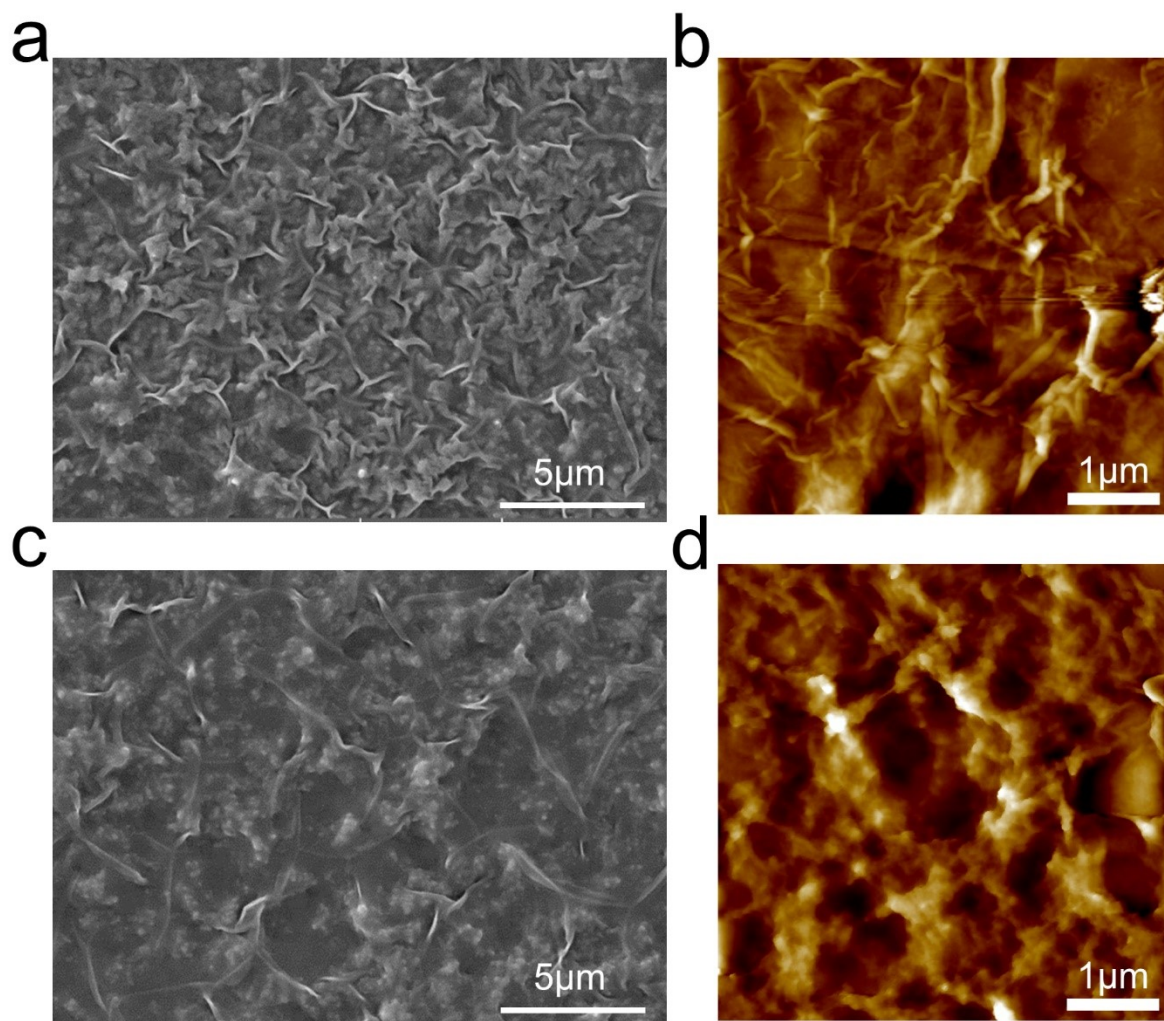


Figure S7. Additional SEM images showing the surface morphology of (a, b) D-*i*TFC-1% and (c, d) D-*i*TFC-0.05%.

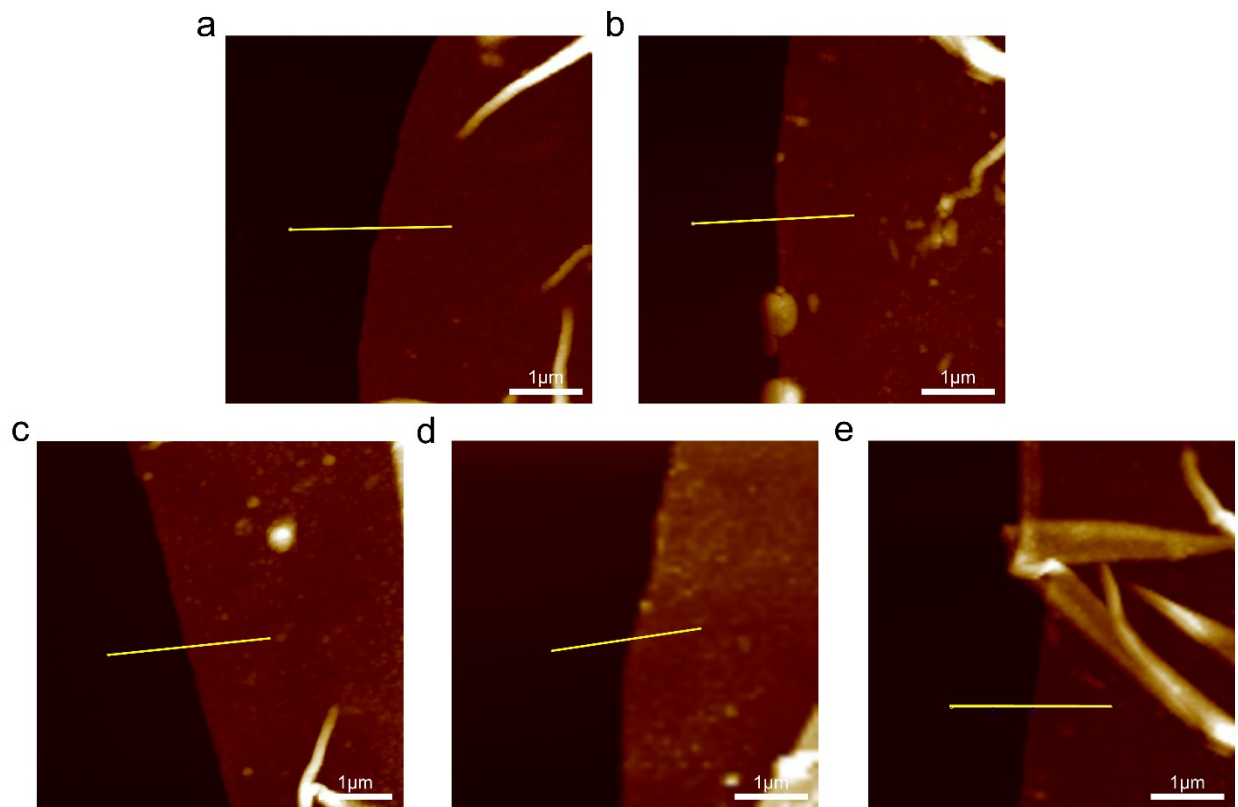


Figure S8. PA films supported on silicon wafers for thickness measurements.

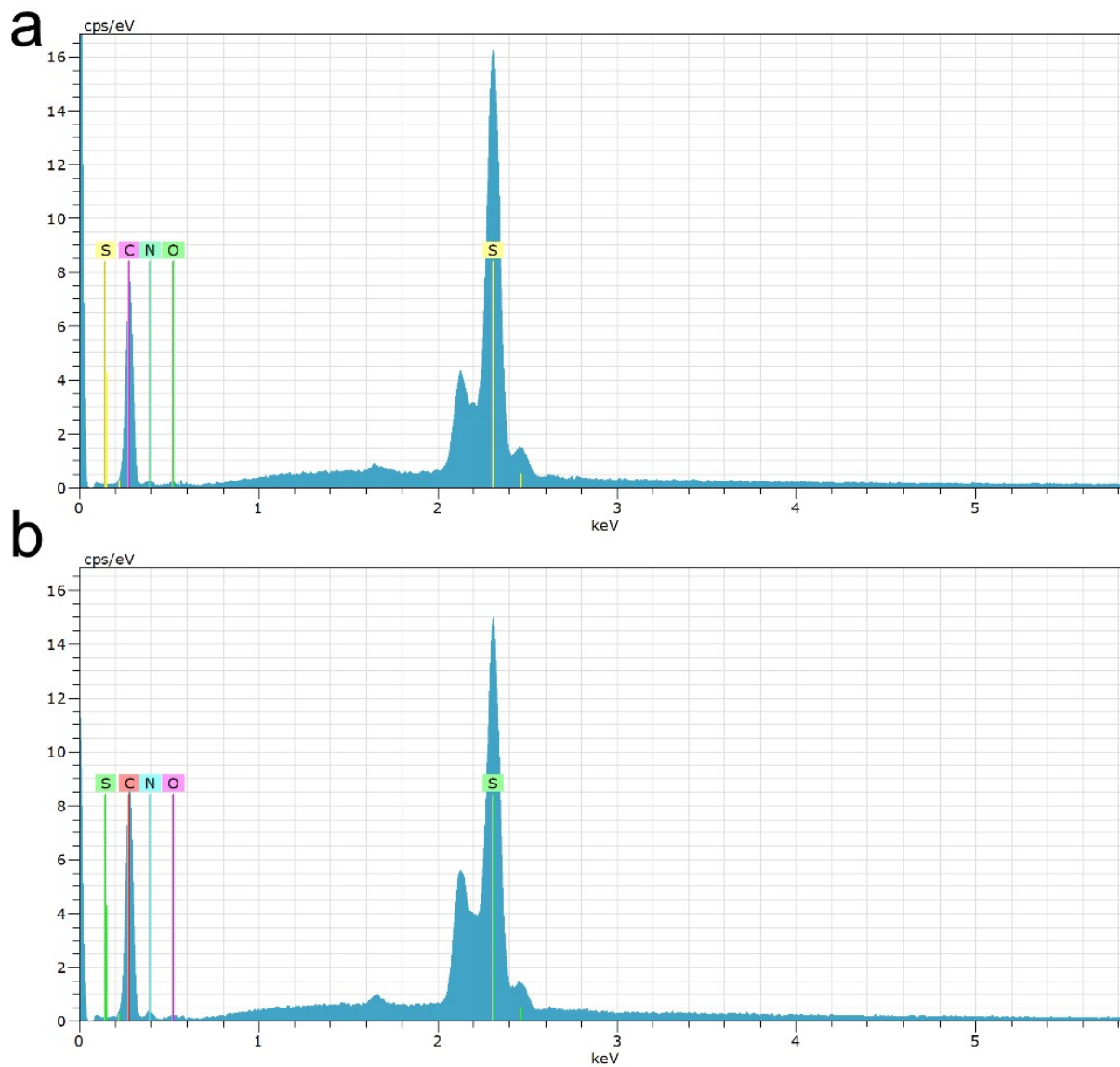


Figure S9. Elemental mapping of the positions marked with a red dot.

Table S1. EDX Elemental Distributions from **Fig. S9a**

EL	AN	Series	Unn. [wt.%]	C norm. [wt.%]	C Atom. [at.%]
C	6	K-series	26.47	66.58	81.02
S	16	K-series	10.66	26.82	12.22
N	7	K-series	2.20	5.54	5.78
O	8	K-series	0.42	1.07	0.97
Total:			39.76	100.00	100.00

Table S2. EDX Elemental Distributions from **Fig. S9b**

EL	AN	Series	Unn. [wt.%]	C norm. [wt.%]	C Atom. [at.%]
C	6	K-series	25.45	67.62	80.70
S	16	K-series	8.92	23.69	10.59
N	7	K-series	2.74	7.29	7.46
O	8	K-series	0.53	1.41	1.26
Total:			37.64	100.00	100.00

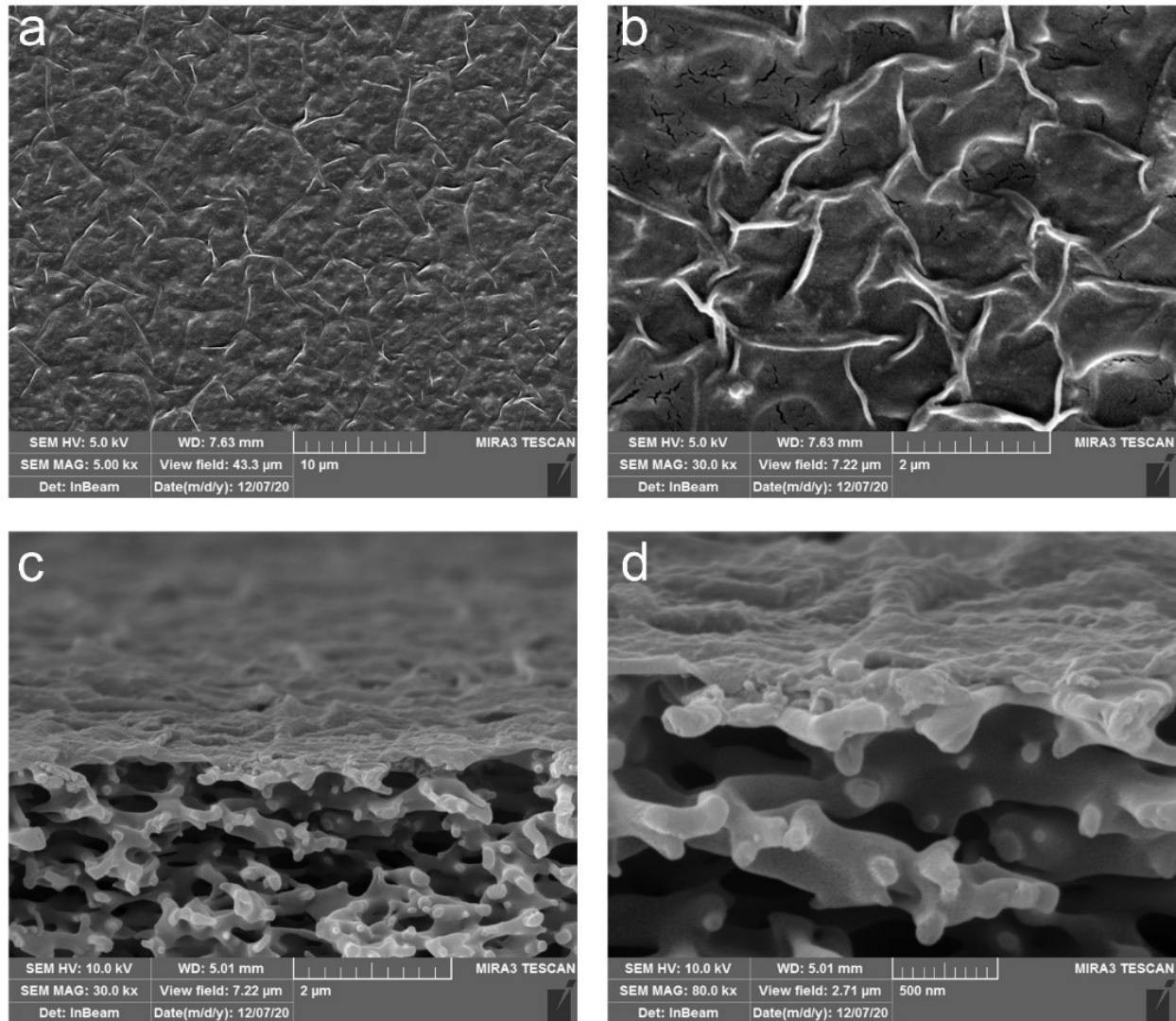


Figure S10. Surface and cross-sectional morphology of an *i*TFC membrane with the PANI interlayer prepared using a 2 mg cm^{-2} loading of PANI nanofibers.

Fig. S10 presents the membrane morphology (1% w/v PIP concentration) of the undoped interlayer built with a reduced areal loading of 2 mg cm^{-2} , the result indicates that the formation of the nanostructured PA layer can also be achieved with a varied thickness of the PANI interlayer.

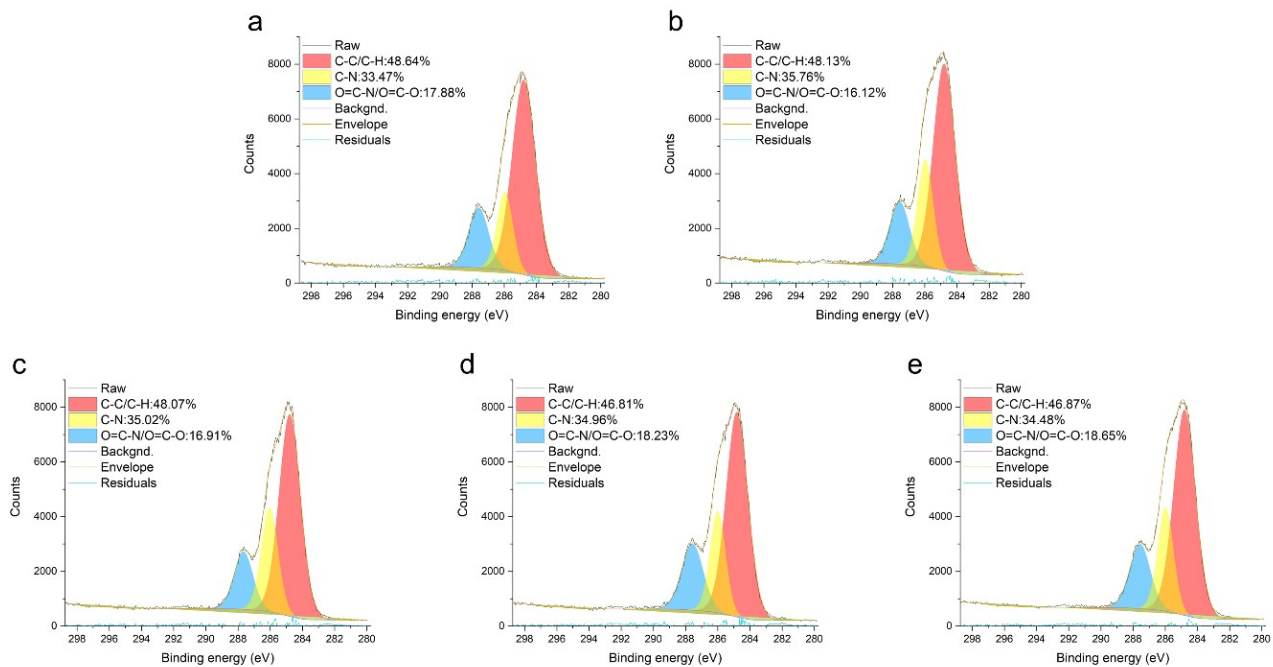


Figure S11. C1s high resolution XPS spectra of TFC-C, U-*i*TFC-1%, D-*i*TFC-1%, U-*i*TFC-0.05%, and D-*i*TFC-0.05% in sequence.

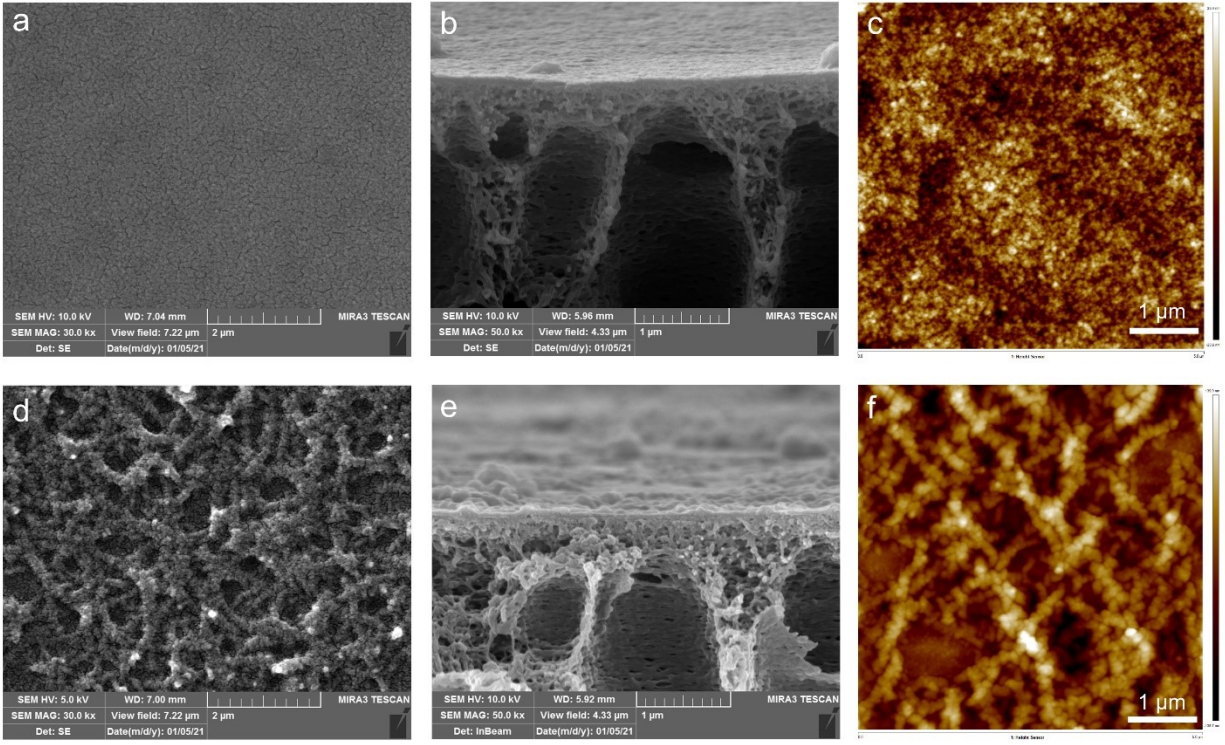


Figure S12. Surface and cross-sectional morphology of (a, b, c) TFC-C-UF and (d, e, f) U-iTFC-1%-UF.

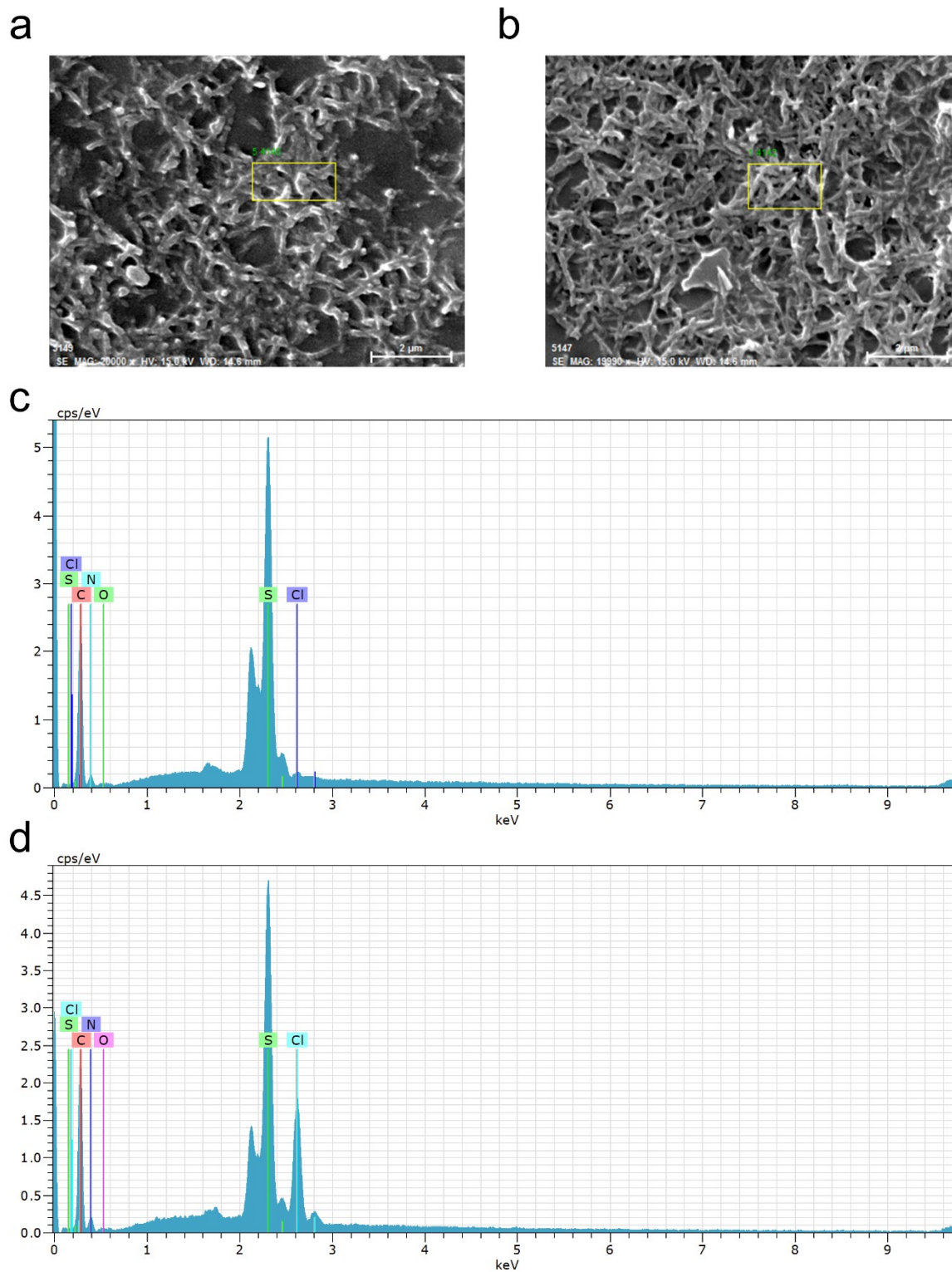


Figure S13. EDX measurement of (a) emeraldine base and (b) emeraldine salt PANI nanofibers with (c) and (d) as the elemental mapping, respectively.

Table S3. Elemental Distribution of Emeraldine Base PANI Nanofibers

EL	AN	Series	Unn. [wt.%]	C norm. [wt.%]	C Atom. [at.%]
C	6	K-series	21.87	62.62	76.01
S	16	K-series	8.54	24.45	11.11
N	7	K-series	3.83	10.97	11.41
O	8	K-series	0.45	1.30	1.19
Cl	17	K-series	0.23	0.67	0.27
Total:			34.93	100.00	100.00

Table S4. Elemental Distribution of Emeraldine Salt PANI Nanofibers

EL	AN	Series	Unn. [wt.%]	C norm. [wt.%]	C Atom. [at.%]
C	6	K-series	29.01	59.87	74.76
S	16	K-series	9.22	19.03	8.90
N	7	K-series	5.16	10.65	11.40
O	8	K-series	0.49	1.01	0.95
Cl	17	K-series	4.58	9.44	3.99
Total:			48.46		

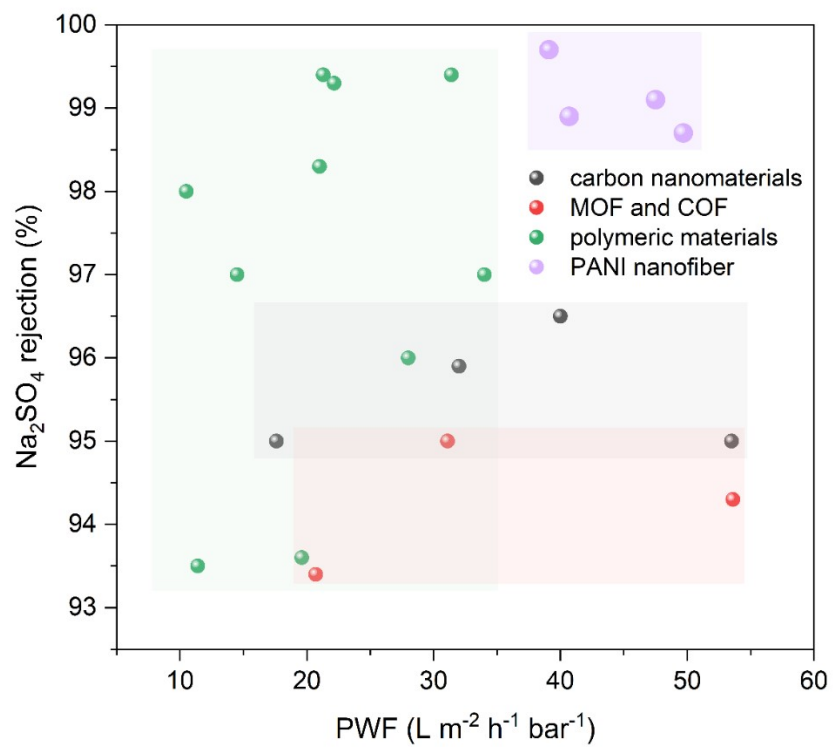


Figure S14. A comparison of Na₂SO₄ rejection and PWF of *i*TFC membranes with PANI interlayers in this work to *i*TFC membranes with other materials-based interlayers.

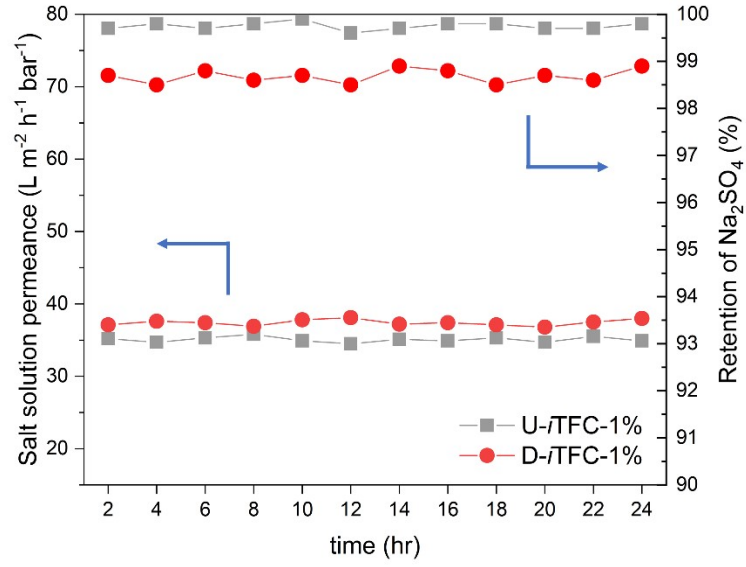


Figure S15. Long-term stability test of nanofiltration. Test conditions: 2,000 ppm Na₂SO₄ solution, 0.5 MPa, 25 °C.